

*Acoustics 2023 Sydney***185th Meeting of the Acoustical Society of America**

Sydney, Australia

4-8 December 2023

Speech Communication: Paper 3pSC4**The influence of sensor size on experimental measurement accuracy of vocal fold contact pressure****Zhaoyan Zhang***Department of Head and Neck Surgery, University of California Los Angeles, Los Angeles, CA, 90095; zyzhang@ucla.edu*

The vocal folds experience repeated collision during phonation. The resulting contact pressure is often considered to play an important role in vocal fold injury, and has been the focus of many experimental studies. In this study, vocal fold contact pattern and contact pressure during phonation were numerically investigated. The results show that vocal fold contact in general occurs within a horizontal strip on the medial surface, first appearing at the inferior medial surface and propagating upward. Because of the localized and traveling nature of vocal fold contact, sensors of a finite size may significantly underestimate the peak vocal fold contact pressure, particularly for vocal folds of low transverse stiffness. This underestimation also makes it difficult to identify the contact pressure peak in the intraglottal pressure waveform. These results showed that the vocal fold contact pressure reported in previous experimental studies may have significantly underestimated the actual values. It is recommended that contact pressure sensors with a diameter no greater than 0.4 mm are used in future experiments to ensure adequate accuracy in measuring the peak vocal fold contact pressure during phonation.

1. INTRODUCTION

During human phonation, the vocal folds experience repeated collision as the glottis periodically opens and closes. The resulting contact pressure between the two vocal folds is often considered an important factor contributing to vocal fold injury (Titze, 1994; Zhang, 2021a). Many research studies have aimed to quantify the magnitude of the contact pressure at different physiological conditions. Direct measurement of vocal fold contact pressure has been attempted in excised larynx experiments (Jiang and Titze, 1994; Mehta et al., 2019; Scheible et al., 2021), physical vocal fold models (Chen & Mongeau, 2011; Weiss et al., 2013; Motie-Shirazi et al., 2019), and human subjects (Hess et al., 1998; Verdolini et al., 1999; Gunter et al., 2005). There are, however, limitations with these experimental studies. For example, due to the invasive nature of the contact pressure sensors, the placement of sensor often leads to discomfort in human subjects and may lead to undesired adjustments in their voice production. The placement of sensors in between the two vocal folds may also interfere with the glottal flow and vocal fold vibration.

In this study, we focus on another limitation associated with the finite size of contact pressure sensors. Due to their finite size, contact pressure sensors measure the contact pressure averaged over the sensing area. Thus, if the sensor size is not small enough to resolve the spatial distribution of the contact pressure, experimental measurement may underestimate the peak vocal fold contact pressure. Table 1 summarizes the sensor dimensions in previous experimental studies, which range from about 0.5 mm to as large as 15mm. Compare these with the typical dimension of the medial surface, which is about 10-17 mm in the anterior-posterior direction and about 2-3 mm in the vertical dimension. It is likely that the relatively large size of the sensors used in these experimental studies may have significantly underestimated the vocal fold contact pressure.

The goal of this study is to evaluate the degree of underestimation in vocal fold contact pressure due to the finite sensor size, and provide some recommendations on selecting sensors for future experimental studies. Because it is difficult to experimentally map out the contact pressure distribution over the vocal fold medial surface, in this study we used contact pressure data generated from voice simulations using a three-dimensional voice production model (Zhang, 2015, 2016, 2017, 2019) as the ground truth. These data were then spatially averaged over a small area to simulate experimental measurement of the vocal fold contact pressure using pressure sensors of varying diameter. We will show that the sensor size used in previous experimental studies can lead to an underestimation of the peak vocal fold contact pressure as large as 87%, depending on the specific vocal fold vibration pattern. It is recommended that sensors with a diameter no greater than 0.4 mm are used in future experiments to ensure adequate accuracy in measuring the peak vocal fold contact pressure.

Table 1: Sensor dimensions in previous experimental studies of vocal fold contact pressure.

Study	Sensor dimension	Study	Sensor dimension
Jiang & Titze, 1994	<7mm ² (~3 mm diameter)	Weiss et al., 2013	0.5 mm x 3 mm
Hess et al., 1998; Verdolini et al., 1999	1.8mm diameter	Motie-Shirazi et al., 2019; Mehta et al., 2019	1 mm x 1 mm
Gunter et al., 2005	10 mm x 15 mm	Scheible et al., 2021	2 mm x 2 mm
Chen & Mongeau, 2011	~0.51 mm diameter		

2. METHODS

The three-dimensional voice production model developed in our previous studies (Zhang, 2015, 2016, 2017, 2019) was used in this study. Details of the model can be found in these past studies. This model has been used in previous studies to investigate the dependence of vocal fold contact pressure on vocal fold geometry, vocal fold stiffness, subglottal pressure (Zhang, 2019, 2020), and vocal tract shape (Zhang, 2021b). These simulations generated voices of varying voice quality, ranging from breathy, modal, to pressed, including both regular and irregular vocal fold vibration (Zhang, 2016, 2018). In particular, these studies showed that the subglottal pressure and the vocal fold transverse stiffness in the coronal plane are the two most important factors determining the magnitude of vocal fold contact pressure (Zhang, 2019).

Pressure sensors often do not distinguish pressure due to vocal fold contact from airflow pressure. Thus, when placed within the glottis, pressure sensors measure the intraglottal pressure, with contributions from both

vocal fold contact and air flow. In this study, the intraglottal pressure was calculated to be the vocal fold contact pressure when there was contact at the specific location or the air pressure when no contact was made. The peak intraglottal pressure was then calculated for each location over the medial surface, and used as the ground truth to evaluate the effect of pressure sensor size on the measurement accuracy.

To simulate experimental measurement of the vocal fold contact pressure, for each location on the medial surface, the intraglottal pressure calculated above was averaged over a neighboring area within a specific radius, simulating the averaging effect of a circular pressure sensor. In this study, four sensor diameters were considered, from 0.5, 1, 2, to 3 mm, roughly corresponding to the lower range of the sensor size used in previous experimental studies (Table 1).

3. RESULTS

Fig. 1 shows the vocal fold contact pressure distribution over the medial surface for twelve instants equally spaced within one cycle of vocal fold vibration, for a condition with a vocal fold thickness $T = 3$ mm, vocal fold transverse stiffness $E_t = 4$ kPa, and subglottal pressure $P_s = 1.2$ kPa. Vocal fold contact initiates in the inferior-anterior region and gradually spreads posteriorly and propagates superiorly. The vertical span of the fully-developed region of vocal fold contact (e.g., instants 6 and 7) is about 0.3 mm in this case. The peak vocal fold contact pressure decreases as the contact propagates superiorly.

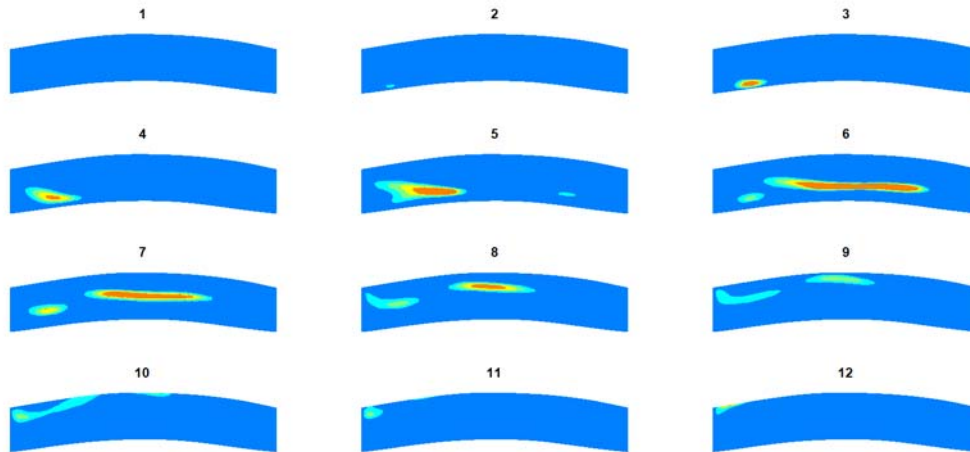


Figure 1: Vocal fold contact pressure over the medial surface for twelve instants equally spaced within one cycle of vocal fold vibration. $T = 3$ mm, $E_t = 4$ kPa, $P_s = 1.2$ kPa, and initial glottal angle $\alpha = 1.6^\circ$. Brighter colors indicate higher vocal fold contact pressure. The medial surface is oriented so that the left-right direction in the figure corresponds to anterior-posterior.

The top panel in Figure 2 shows the peak intraglottal pressure over the medial surface. In this case, the peak intraglottal pressure distribution shows two regions of high peak vocal fold contact pressure along the vertical direction, due a low mucosal wave speed. The dominant region occurred at the inferior medial surface and a second region with a relatively weaker peak vocal fold contact pressure can be observed at a more superior location. Comparison to the vocal fold contact pattern in Figure 1 indicates that these two regions are associated with vocal fold contact rather than intraglottal air pressure.

The other panels of Figure 2 show the peak intraglottal pressure distribution that would be measured in experiments using pressure sensors of varying diameter from 0.5 mm to 3 mm. As expected, increasing sensor diameter reduces the measured peak vocal fold contact pressure. For a sensor diameter of 3 mm, this underestimation of the overall peak vocal fold contact pressure is 59% in this case. Sensors of large size ($d > 0.5$ mm) also fail to identify the second region of high peak vocal fold contact pressure located on the superior portion of the medial surface.

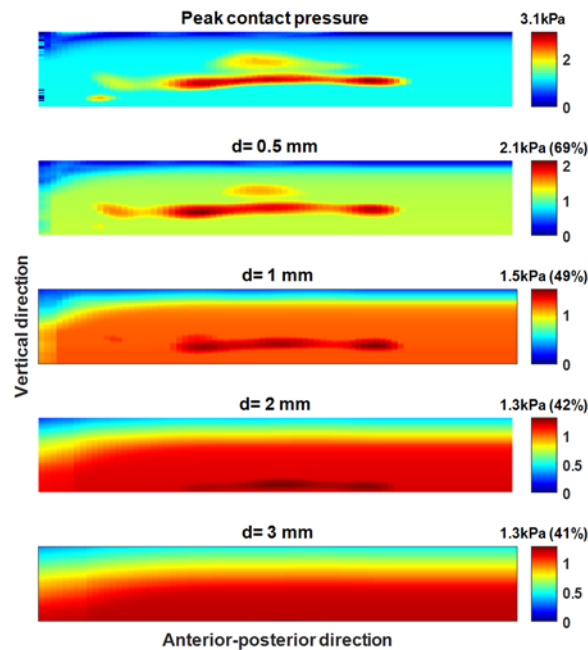


Figure 2: Distribution of the peak intraglottal pressure over the medial surface (top) and the simulated distribution of peak contact pressure measured using sensors of varying diameter. Large sensors significantly underestimate the peak vocal fold contact pressure. $T = 3\text{ mm}$, $E_t = 4\text{ kPa}$, $P_s = 1.2\text{ kPa}$, and initial glottal angle $\alpha = 1.6^\circ$.

Due to this underestimation effect, the measured peak vocal fold contact pressures are more comparable in magnitude to the intraglottal air pressures than they actually are, particularly for large sensors. This can be observed in Figure 2 by the gradually reduced contrast between the regions of high peak vocal fold contact pressure and the intraglottal air pressure in the background. The reduced prominence of the measured contact pressure over the intraglottal air pressure is more clearly illustrated in Figure 3, which shows that the vocal fold contact pressure in the center of the medial surface as a function of time as well as the contact pressure that would be measured using a sensor of varying diameters. With increasing sensor size, the magnitude of the peak associated with vocal fold contact is reduced. For a sensor size larger than 0.5 mm, the measured peak contact pressure is comparable to the peak air pressure, thus making it difficult to identify the contact pressure peak in the intraglottal pressure waveform.

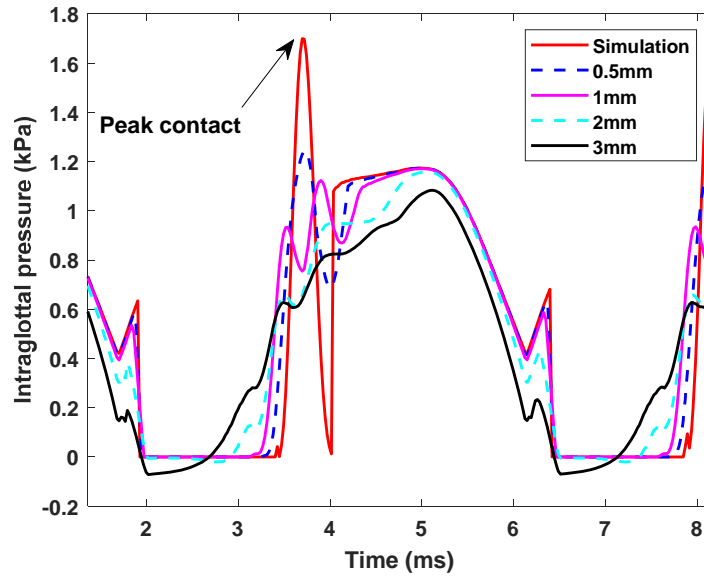


Figure 3: Vocal fold contact pressure in the center of the medial surface as a function of time, and the contact pressure that would be measured using a sensor of varying diameters. The prominence of the peak contact pressure diminishes with increasing sensor diameter. $T = 3\text{mm}$, $E_t = 4\text{ kPa}$, $P_s = 1.2\text{ kPa}$, and initial glottal angle $\alpha = 1.6^\circ$.

The degree of underestimation in the peak contact pressure appears to increase with the magnitude of the peak contact pressure. Figures 4 and 5 show similar data for a vocal fold configuration with a much stronger vocal fold contact, due to a lower transverse stiffness ($E_t = 1\text{ kPa}$) of the vocal folds and thus much higher vocal fold vibration amplitude. In this case, due to the reduced wave speed, two regions of strong peak contact pressure can be observed in the peak intraglottal pressure distribution over the medial surface (Figure 5). Comparison to the contact pressure in Figure 4 indicates that these peaks are associated with vocal fold contact pressure. The overall peak vocal fold contact pressure was around 18 kPa, which is much higher than those reported in previous experiments. However, the degree of underestimation is also much higher than that in Figure 2, reaching about 87% for a sensor diameter of 3mm. As a result, despite a very high overall peak contact pressure of 18 kPa, the value that would be measured by a sensor of 2mm diameter is about 3.1 kPa, much closer to the typical range reported in previous experimental studies.

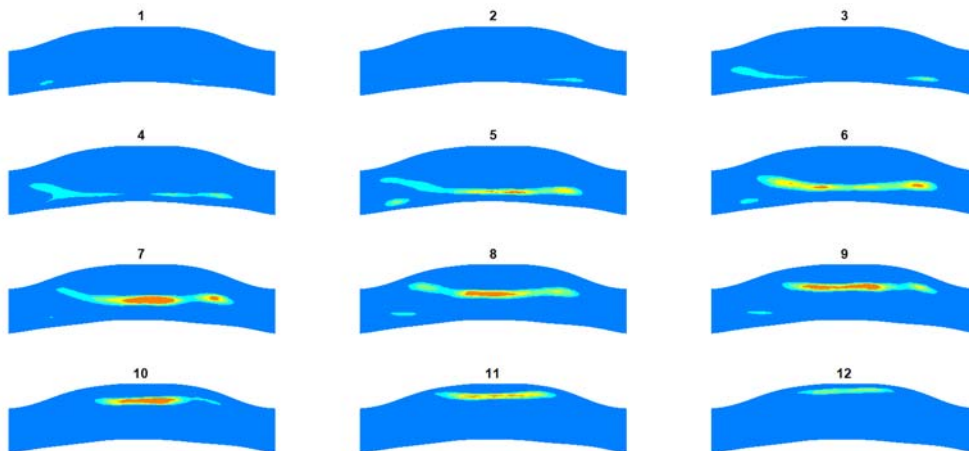


Figure 4: Condition with strong vocal fold contact. Vocal fold contact pressure over the medial surface for twelve instants equally spaced within one cycle of vocal fold vibration. $T = 3\text{mm}$, $E_t = 1\text{ kPa}$, $P_s = 1.2\text{ kPa}$, and initial glottal angle $\alpha = 1.6^\circ$. Brighter colors indicate higher vocal fold contact pressure. The medial surface is oriented so that the left-right direction in the figure corresponds to anterior-posterior.

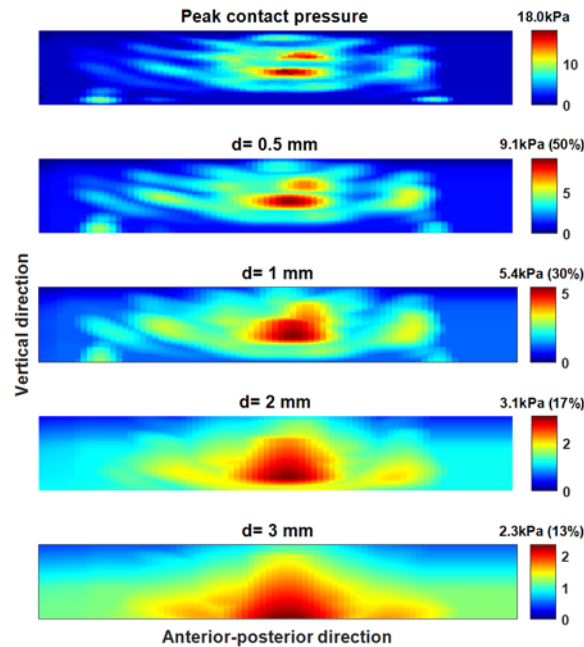


Figure 5: Condition with strong vocal fold contact. Distribution of the peak intraglottal pressure over the medial surface (top) and the simulated distribution of peak contact pressure measured using sensors of varying diameter. Large sensors significantly underestimate the peak vocal fold contact pressure. $T = 3\text{ mm}$, $E_t = 1\text{ kPa}$, $P_s = 1.2\text{ kPa}$, and initial glottal angle $\alpha = 1.6^\circ$.

It is worth noting that the underestimation mainly applies to the vocal fold contact pressure but not much to the intraglottal air pressure. As an example, Figure 6 shows the peak intraglottal pressure over the medial surface for a condition with minimal vocal fold contact, in which the intraglottal pressure has contributions mainly from the intraglottal air pressure. In this case, use of large sensors leads to only slight underestimation of the peak intraglottal air pressure, about 9% for a sensor diameter of 3 mm. The overall intraglottal air pressure distribution is qualitatively preserved even for the largest sensor diameter.

This differential effect of sensor size on the vocal fold contact pressure and intraglottal air pressure is due to the difference in spatial distribution. Because vocal fold contact often occurs along a narrow, horizontal strip with a vertical width in the order of 0.4 mm, outside of which the contact pressure is zero, averaging tends to significantly underestimate the peak contact pressure. In contrast, the air pressure distribution varies relatively more gradually, thus a smaller effect of spatial averaging.

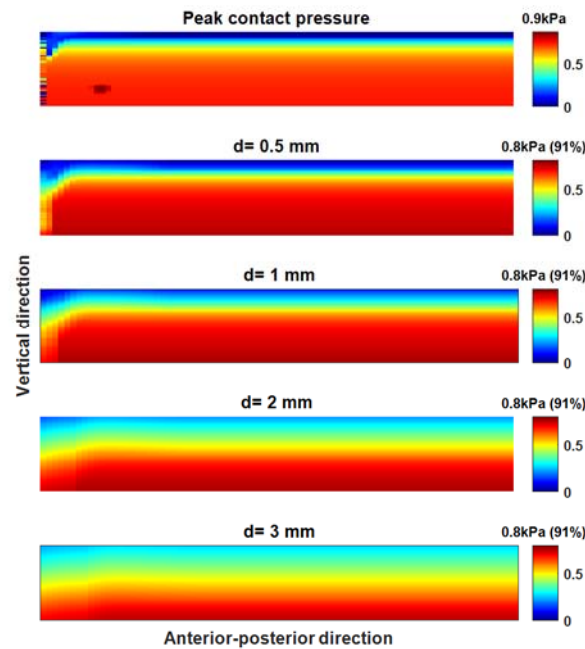


Figure 6: Conditions with minimal vocal fold contact. Distribution of the peak intraglottal pressure over the medial surface (top) and the simulated distribution of peak contact pressure measured using sensors of varying diameter. Large sensors significantly underestimate the peak vocal fold contact pressure. $T = 2\text{mm}$, $E_t = 4\text{ kPa}$, $P_s = 0.8\text{ kPa}$, and initial glottal angle $\alpha = 1.6^\circ$.

4. DISCUSSION AND CONCLUSIONS

Our results showed that vocal fold contact often initiates at the inferior portion of the vocal fold medial surface as a narrow, horizontal strip and propagates superiorly. The vertical span of the contact pressure is in the order of 0.3-0.4 mm. As a result, to adequately resolve the vocal fold contact pressure spatially, pressure sensors with a sensing diameter no greater than 0.4 mm should be used in experiments.

Because vocal fold contact often occurs along a narrow, horizontal strip, the vocal fold contact pressure varies more abruptly along the vertical direction than the anterior-posterior direction. Thus, it is important to scan the vocal fold contact pressure with a much finer spatial resolution along the vertical direction (e.g., about 0.1 mm), whereas the spatial resolution along the anterior-posterior direction is less critical.

An important finding of this study is that larger sensors may significantly underestimate the peak vocal fold contact pressure, by as large as 87% for a sensor diameter of 3 mm. This underestimation also makes it difficult to identify the contact pressure peak in the intraglottal pressure waveform. Since previous experimental studies often used a sensor size much larger than 0.4 mm, our results suggest that the vocal fold contact pressure reported in those previous experimental studies may have significantly underestimated the actual values.

ACKNOWLEDGMENTS

This study was supported by research grant R01 DC020240 from the National Institute on Deafness and Other Communication Disorders, the National Institutes of Health.

REFERENCES

- Chen, L., and Mongeau, L. (2011). "Verification of two minimally invasive methods for the estimation of the contact pressure in human vocal folds during phonation," *J. Acoust. Soc. Am.* 130, 1618-1627.
- Gunter, H. E., Howe, R., Zeitels, M., Kobler, J. B., and Hillman, R. (2005). "Measurement of vocal fold collision forces during phonation: Methods and preliminary data," *J. Speech, Lang., Hear. Res.* 48, 567-576.
- Hess, M. M., Verdolini, K., Bierhals, W., Mansmann, U., and Gross, M. (1998). "Endolaryngeal contact pressures," *J. Voice* 12, 50-67.

-
- Jiang, J. J., and Titze, I. R. (1994). "Measurement of vocal fold intraglottal pressure and impact stress," *J. Voice* 8(2), 132-144.
- Mehta, D. D., Kobler, J. B., Zeitels, S. M., Zañartu, M., Erath, B. D., Motie-Shirazi, M., ... & Hillman, R. E. (2019). "Toward development of a vocal fold contact pressure probe: Bench-top validation of a dual-sensor probe using excised human larynx models," *Applied Sciences*, 9(20), 4360.
- Motie-Shirazi, M., Zañartu, M., Peterson, S. D., Mehta, D. D., Kobler, J. B., Hillman, R. E., & Erath, B. D. (2019). "Toward development of a vocal fold contact pressure probe: Sensor characterization and validation using synthetic vocal fold models," *Applied Sciences*, 9(15), 3002.
- Scheible, F., Veltrup, R., Schaan, C., Lamprecht, R., Staggl, M., Semmler, M., & Sutor, A. (2021). "Measuring contact pressures of phonating vocal fold using a pressure-sensing-matrix during hemi-larynx experiments," In *Proceedings of Meetings on Acoustics*, Vol. 45, No. 1, 060007.
- Titze, I. R. (1994). "Mechanical stress in phonation," *J. Voice* 8, 99105.
- Verdolini, K., Hess, M. M., Titze, I. R., Bierhals, W., and Gross, M. (1999). "Investigation of vocal fold impact stress in human subjects," *J. Voice* 13, 184-202.
- Weiss, S., Sutor, A., Rupitsch, S. J., Kniesburges, S., Doellinger, M., & Lerch, R. (2013). "Development of a small film sensor for the estimation of the contact pressure of artificial vocal folds," *Proc. Mtgs. Acoust.* 19, 060307.
- Zhang, Z. (2015). "Regulation of glottal closure and airflow in a three-dimensional phonation model: Implications for vocal intensity control," *J. Acoust. Soc. Am.*, 137(2), 898-910.
- Zhang, Z. (2016). "Cause-effect relationship between vocal fold physiology and voice production in a three-dimensional phonation model," *J. Acoust. Soc. Am.* 139, 1493–1507.
- Zhang, Z. (2017). "Effect of vocal fold stiffness on voice production in a three-dimensional body-cover phonation model," *J. Acoust. Soc. Am.*, 142(4), 2311–2321.
- Zhang, Z. (2018). "Vocal instabilities in a three-dimensional body-cover phonation model," *J. Acoust. Soc. Am.*, 144(3), 1216–1230.
- Zhang, Z. (2019). "Vocal fold contact pressure in a three-dimensional body-cover phonation model," *J. Acoust. Soc. Am.*, 146(1), 256-265.
- Zhang, Z. (2020). "Laryngeal strategies to minimize vocal fold contact pressure and their effect on voice production," *J. Acoust. Soc. Am.*, 148, 1039-1050.
- Zhang, Z. (2021a). "The physical aspects of vocal health," *Acoustics Today*, 17(3), 60-68.
- Zhang, Z. (2021b). "Interaction between epilaryngeal and laryngeal adjustments in regulating vocal fold contact pressure," *JASA Express Letters*, 1(2), 025201.